An assessment of the tracer-based approach to quantifying groundwater contributions to streamflow

J. P. Jones, E. A. Sudicky, A. E. Brookfield, and Y.-J. Park

Department of Earth Sciences, University of Waterloo, Waterloo, Ontario, Canada

Received 22 March 2005; revised 11 October 2005; accepted 8 November 2005; published 18 February 2006.

[1] The use of conservative geochemical and isotopic tracers along with mass balance equations to determine the pre-event groundwater contributions to streamflow during a rainfall event is widely used for hydrograph separation; however, aspects related to the influence of surface and subsurface mixing processes on the estimates of the pre-event contribution remain poorly understood. Moreover, the lack of a precise definition of "pre-event" versus "event" contributions on the one hand and "old" versus "new" water components on the other hand has seemingly led to confusion within the hydrologic community about the role of Darcian-based groundwater flow during a storm event. In this work, a fully integrated surface and subsurface flow and solute transport model is used to analyze flow system dynamics during a storm event, concomitantly with advective-dispersive tracer transport, and to investigate the role of hydrodynamic mixing processes on the estimates of the pre-event component. A number of numerical experiments are presented, including an analysis of a controlled rainfall-runoff experiment, that compare the computed Darcian-based groundwater fluxes contributing to streamflow during a rainfall event with estimates of these contributions based on a tracer-based separation. It is shown that hydrodynamic mixing processes can dramatically influence estimates of the pre-event water contribution estimated by a tracer-based separation. Specifically, it is demonstrated that the actual amount of bulk flowing groundwater contributing to streamflow may be much smaller than the quantity indirectly estimated from a separation based on tracer mass balances, even if the mixing processes are weak.

Citation: Jones, J. P., E. A. Sudicky, A. E. Brookfield, and Y.-J. Park (2006), An assessment of the tracer-based approach to quantifying groundwater contributions to streamflow, *Water Resour. Res.*, *42*, W02407, doi:10.1029/2005WR004130.

1. Introduction

[2] Separating event (precipitation) from pre-event (unsaturated- and saturated-zone subsurface) contributions to streamflow during rainstorms remains a common focus of hydrological studies. One widely employed separation method involves using conservative geochemical or isotopic tracers [e.g., *Christophersen et al.*, 1990; *Hooper et al.*, 1990; *Christophersen and Hooper*, 1992; *Brown et al.*, 1999; *Hooper*, 2001; *Hooper*, 2003]; however, *Rice and Hornberger* [1998] have shown that the source zones contributing to streamflow generation cannot be unambiguously identified using tracer measurements interpreted with mass balance equations alone. Moreover, results generated using tracer-based separation techniques are sometimes viewed as being paradoxical because they commonly show pre-event waters originating from the subsurface to be a major contributor to the observed rise in stream discharge shortly after a rainstorm, although subsurface Darcian-type flow is usually considered to be a relatively slow process. The question then arises as to how this subsurface pre-event water can be transmitted so rapidly to the stream channel.

[3] Most tracer-based studies, whether they consist of two-, three-, or more component conceptual models, utilize mass balance equations to perform the hydrograph separation. The mass balance equations, in their three-component form, can be written as

$$Q_t = Q_p + Q_u + Q_s \tag{1a}$$

$$C_{ti}Q_t = C_{pi}Q_p + C_{ui}Q_u + C_{si}Q_s \qquad i = 1, 2 \tag{1b}$$

where Q [L^3/T] is discharge, C [M/L^3] is concentration, and the subscripts t, p, u, and s refer to the total flow as measured in the stream, the surface runoff component arising directly from the precipitation event, the pre-event unsaturated zone portion, and the pre-event component from the saturated zone, respectively. If the initial concentrations of each tracer originating from the precipitation, unsaturated, and saturated zones (C_{pi}, C_{ui}, and C_{si}) are known a priori and their values are measured over time in the stream (C_{ti}), then the tracer mass balance relationships given by equations (1a) and (1b) are presumed to provide estimates of the unknown source-zone contributions (Q_p, Q_u, and Q_s) to the total discharge (Q_t).

[4] We note that the Q values appearing in (1a) and (1b) are typically interpreted by most hydrologists to mean a

0043-1397/06/2005WR004130

Table 1. Results of Previous Two-Component Tracer-Based Hydrograph Separation Studies[a]

Reference	Catchment Area, km^2	Tracer	Geological Setting	Pre-Event Contribution to Total Discharge Volume, %
Jordan [1994]	0.036	^{18}O	shallow soils	45, 75
McDonnell et al. [1990]	3.1	D	...	24
Fritz et al. [1976]	22	^{18}O	clay-loam glacial till	90
Fritz et al. [1976]	1.8	^{18}O	shallow sands, silts, and clays	40–45
McGlynn and McDonnell [2003]	0.0264	^{18}O	silt loams	53–96
Buttle and Peters [1997]	0.0322	^{18}O	sandy till	77
Hill and Waddington [1993]	1.57	^{18}O	glacial deposits	59–89
Kendall et al. [2001]	0.00049	^{18}O	shallow silty loam	10
Leopoldo and Martinez [1987]	1.58	^{18}O	sandy soils	55–93
Leopoldo and Martinez [1987]	3.27	^{18}O	sandy soils	47–87
Bottomley et al. [1984]	1.24	^{18}O, D	glacial deposits	40
Turner et al. [1987]	0.82	^{18}O, D, Cl	...	60–95
Blowes and Gillham [1988]	0.0075	^{18}O, Cl	fine sands and silts	22–50
Nolan and Hill [1990]	10.6	D	clays, stony loams	57, 89
Crouzet et al. [1970]	0.57	T	...	97
Crouzet et al. [1970]	15	T	...	99
Crouzet et al. [1970]	91	T	...	46
Kennedy et al. [1986]	620	D, T	gravelly to clayey loam	50–80
DeWalle et al. [1988]	2.08	^{18}O	silt loams	75
Loye-Pilot and Jusserand [1990]	0.33	^{18}O	...	60–90
Sklash [1990]	0.038	^{18}O, D	shallow humic soil	75–85
Turner and MacPherson [1990]	27	D	deeply weathered granite	58
Turner et al. [1991]	6	D	shallow soils	25
Turner et al. [1991]	10	D	shallow soils	37
Abdul and Gillham [1989]	0.1	Br	medium sands	37

[a]D, deuterium; T, tritium; ^{18}O, oxygen-18; Br, bromide.

bulk, hydraulic-gradient-driven flow such as, for example, Darcian-type subsurface flow. Implicit in the tracer mass fluxes *CQ* appearing in (1b), however, are the dispersive/diffusive fluxes of each tracer component contained in the water, which are driven by concentration gradients. Even if, for example, there exists a negligible hydraulic gradient between the groundwater system and the stream such that there is little or no bulk groundwater discharge into the stream, the signature of the groundwater tracer appearing in the stream will change over time because of the dispersive/diffusive component of the total flux. Unless this dispersive/diffusive flux is explicitly accounted for in an interpretation based on (1a) and (1b), the water in the stream may appear to be ''old'' even though the advective, hydraulically driven, tracer flux (i.e., pre-event) into the stream may be negligible.

[5] The application of equations (1a) and (1b) seems reasonable for hydrologic conditions where the degree of mixing between the event and pre-event waters is negligible. If this is indeed the case, one can presume that it would yield a hydrograph separation that accurately reflects the actual relative contributions of the various source-zone waters to streamflow generation as driven by hydraulic gradients, whether they be overland- or subsurface-based flow rules describing the bulk flow of the aqueous (i.e., water) phase. However, in situations where the degree of mixing between event and pre-event waters is nonnegligible (presumably a common situation), the application of mass balance equations such as (1a) and (1b) to interpret the chemograph produced in the stream by the tracers raises some concerns. For instance, a number of previous tracer-based separation studies that used mass-balance relationships have concluded that the pre-event water was a major contributor to streamflow generation during a storm event (Table 1), even though Darcian groundwater flow is usually considered to be a relatively slow process. In the past, a number of mechanisms have been proposed to explain the apparent discrepancies between the conventional understanding of watershed flow dynamics and results produced by tracer-based separation studies interpreted with the mass balance equations. For example, a commonly proposed mechanism to explain the rapid mobilization of subsurface flow involves the role of macropores of various types, sizes, and frequencies [see, e.g., *Weiler and Naef*, 2003]. While the presence of macropores can certainly enhance subsurface contributions to streamflow, these features were not noted in several of the case studies reported in Table 1.

[6] A more parsimonious explanation may be that each component's tracer signature is being altered in ways not accounted for by the standard application of a mass balance equation such as that given by (1b), which lumps the advective and dispersive/diffusive fluxes, thereby affecting the interpretation of the tracer study's chemograph at some time *t*. This has been demonstrated to be the case by *Chanat and Hornberger* [2003] for flow components that mix within the near-stream zone although they did not use a dynamic and fully integrated surface-subsurface flow and transport model that explicitly accounts for dispersion processes. Similarly, *Burt* [2005] has recently suggested that the tracer signatures measured in the stream may be affected by residence time and changing conditions along the flow path. Factors that can affect the strength of the hydrodynamic mixing occurring between the component waters include mechanical dispersion, molecular diffusion, and rainfall intensity/duration.

[7] The main objectives of this work are (1) to quantify the influence of the dispersive/diffusive mixing of tracer signatures for the precipitation, unsaturated-zone and saturated-zone waters along both the surface and subsurface flow paths, (2) to demonstrate how the changing signatures along the flow paths can influence tracer-based estimates of the pre-event subsurface contribution to streamflow during a precipitation event, and (3) to compare tracer-based, pre-event subsurface contributions estimated from the traditional mass balance approach with bulk flow quantities calculated on the basis of hydraulic-gradient-driven flow processes. To achieve these objectives, a fully integrated surface/variably saturated subsurface flow and mass transport model will be applied to a conceptual example in addition to a controlled rainfall-runoff experiment conducted by *Abdul* [1985] at a site located at Canadian Forces Base Borden [see also *Abdul and Gillham*, 1989]. The integrated hydrology model InHM [*VanderKwaak*, 1999], originally developed at the University of Waterloo, is a fully coupled control-volume finite element model which can simulate water flow and advective-dispersive solute transport over the two-dimensional land surface and in the three-dimensional subsurface under variably saturated conditions. Full coupling of the surface and subsurface flow regimes is accomplished by simultaneously solving one system of nonlinear discrete equations describing flow and tracer transport in both flow regimes, as well as the water and solute fluxes between continua. Because the model is fully coupled and fully integrated, all components of the flow system, including water exchanged between the surface and subsurface hydrologic regimes, can be directly computed and compared with results calculated by simulating advective-dispersive tracer transport and then applying the mass balance equations (1a) and (1b) to interpret the tracer-based chemograph. Details concerning the theory, numerical solution techniques, and example applications of the InHM model are given by *VanderKwaak* [1999] and *VanderKwaak and Loague* [2001].

2. The Paradox of the Rapid Mobilization of Old Water

[8] Table 1 is a compilation of estimates of pre-event groundwater contributions to rainstorm-induced streamflow based on the use of tracers. The data were drawn from the literature and build upon previous compilations presented by *Jordan* [1994], *Turner and Barnes* [1998], and *Genereux and Hooper* [1998]. As can be seen in Table 1, the estimates of the pre-event contribution commonly exceed 50% and in many cases exceed 75% regardless of the catchment size or the hydrological and geological setting. These findings tend to contradict the conventional physical understanding of the dynamics driving water flow in catchments because saturated and unsaturated subsurface flows are usually thought of as relatively slow processes. Nevertheless, the preponderance of the geochemical evidence points to substantial quantities of pre-event water contributing to streamflow during precipitation. *Kirchner* [2003] has referred to this contradiction as the "rapid mobilization of old water paradox."

[9] A number of physical mechanisms have been proposed in attempts to resolve this paradox, including groundwater ridging or the capillary-fringe effect [*Sklash and Farvolden*, 1979; *Novakowski and Gillham*, 1988; *Abdul and Gillham*, 1989], translatory flow [*Hewlett and Hibbert*, 1967; *Buttle*, 1989; *Bishop et al.*, 1990], and macropore flow [*Mosley*, 1979; *McDonnell*, 1990; *Weiler and Naef*, 2003]. A review by *Buttle* [1994] discusses a number of these and other proposed mechanisms in detail. As *Kirchner* [2003] pointed out, the proposition of a mechanism for the rapid mobilization of pre-event water must be physically plausible and quantitatively realistic. Instead of trying to conform catchment response physics to the geochemical (i.e., tracer) evidence, it might be more useful to examine how physically plausible this evidence actually is.

[10] The capillary-fringe effect merits further discussion due to its relevance to this work. For hydrologic systems with shallow water tables, the possibility exists for the zone of tension saturation (the capillary fringe) to extend from the water table to the land surface particularly in the near-stream environment. In this situation, the addition of a small amount of water would relieve capillary tension and will produce a rapid rise in the water table near the stream that, in turn, increases the hydraulic driving force for the rapid discharge of pre-event water to the stream [*Gillham*, 1984]. This rise in the water table can also manifest itself on the land surface as exfiltration, which presents an opportunity for event and pre-event waters to mix before reaching the stream channel.

[11] Most of the previous attempts at reconciling tracer-based results with the current physical understanding of the dynamics driving streamflow generation assume that the simple mass balance relationships used for interpreting the geochemical data adequately reflect the dynamics of the groundwater and surface water flow regimes, including any mixing that occurs along and between flow paths. However, if the effects of mixing are not adequately reflected by these mass balance relationships, then the Q_p, Q_u, and Q_s terms in equations (1a) and (1b) will not necessarily be equivalent to the actual bulk flow components they purport to represent unless Darcian-type flow is the sole tracer transport mechanism and the hydrodynamic mixing effects of mechanical dispersion and molecular diffusion are negligible. Note that in catchments where both transient advective transport and hydrodynamic mixing processes play a role, which is likely the general situation, all of the bulk flow components contributing to streamflow generation (e.g., surface runoff, subsurface Darcian flow) would be a mixture of event and pre-event waters. Therefore, if the dispersive fluxes and the effects of hydrodynamic mixing on each component's tracer signature are not explicitly accounted for in the mass balance relationships, then as the mixing becomes more active, the correspondence between the Q_u and Q_s terms in equations (1a) and (1b) and the hydraulically driven bulk flow components they are supposed to represent will progressively deteriorate (i.e., an inflation of interpreted Q_u and Q_s values). If this is indeed the case, then there would be no paradox between the conventional understanding of flow system hydrodynamics and tracer-based hydrograph separation data, leaving only the question as to how the tracer data should be interpreted. To explore these hypotheses, the remainder of this paper will focus on determining to what extent hydrodynamic mixing processes might affect an interpretation of

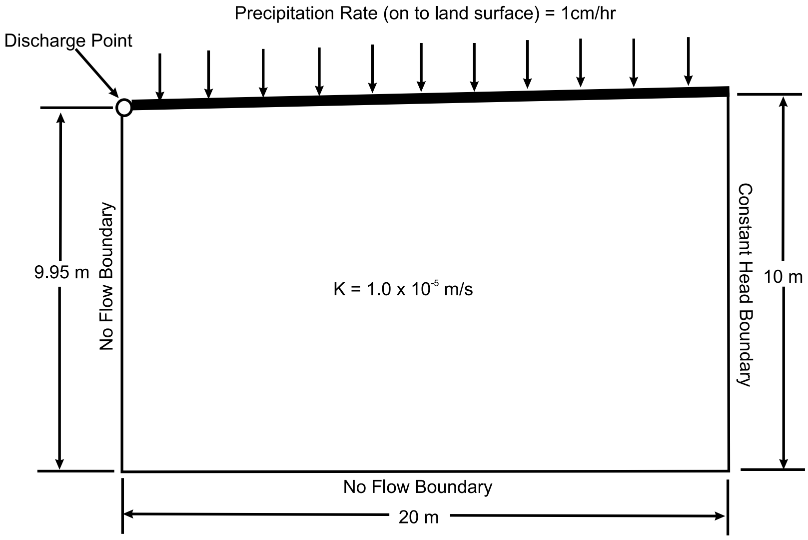

Figure 1. Conceptual hillslope example used to illustrate the effects of hydrodynamic mixing on tracer signatures.

the quantity of event versus pre-event water contributing to streamflow generation, especially if the hydrograph separation is based on a mass balance relation such as (1b).

3. An Illustrative Example of the Influence of Hydrodynamic Mixing on Hydrograph Separation

[12] A hypothetical two-dimensional flow system is used to illustrate how rainfall and groundwater tracer signatures are altered by different degrees of hydrodynamic mixing before discharging into a stream. The hypothetical system is initially saturated to the land surface, is 20 m wide, is 10 m high on the right-hand side, and has a surface slope of 0.0025 (Figure 1). A 10-m specified-head boundary condition was applied to the right-hand side of the system, no flow boundaries were assigned to the bottom and left-hand sides, and a nonlinear critical depth boundary condition was placed at the discharge point. With this boundary condition applied to the outlet, neither the flow nor the water depth is constrained in the InHM model formulation. The control-volume finite element mesh was discretized at a level of 0.04 m horizontally and 0.02 m vertically for a total of 251,001 nodes.

[13] Three scenarios are considered using this hypothetical flow system: (1) a zero-dispersion case, (2) a diffusion-only case, and (3) a high-dispersion case. For each scenario, a 1.0 cm/h rainfall event is applied to the surface for 1 hour and then the system is allowed to equilibrate for an additional 4 hours. Both the groundwater and incoming rainfall are tagged as separate and independent conservative tracers. The groundwater tracer is given an initial concentration of 1.0 and the rainfall concentration is also fixed at 1.0, although its value can change as it falls on the land surface due to dispersive/diffusive exchange processes between the subsurface and surface flow regimes. Table 2 summarizes the surface and subsurface transport parameters used in the three scenarios as well as the hydrological properties assigned to the system. Note that the micro-

Table 2. Model Parameters Used in the Illustrative Example for the Zero-Dispersion, Diffusion-Only, and High-Dispersion Cases

	Zero-Dispersion Case	Diffusion-Only Case	High-Dispersion Case
	Surface		
Manning's surface roughness coefficient	0.001 s/m$^{1/3}$	0.001 s/m$^{1/3}$	0.001 s/m$^{1/3}$
Microtopography height	1×10^{-5} m	1×10^{-5} m	1×10^{-5} m
Mobile water depth	1×10^{-4} m	1×10^{-4} m	1×10^{-4} m
Longitudinal dispersivity	0.0 m	0.0 m	0.1 m
Transverse dispersivity	0.0 m	0.0 m	0.1 m
Molecular diffusion coefficient	1.2×10^{-15} m^2/s	1.2×10^{-9} m^2/s	1.2×10^{-9} m^2/s
	Subsurface		
Porosity	0.37	0.37	0.37
Specific storage	3.2×10^{-4} m^{-1}	3.2×10^{-4} m^{-1}	3.2×10^{-4} m^{-1}
Saturated hydraulic conductivity	1.0×10^{-5} m/s	1.0×10^{-5} m/s	1.0×10^{-5} m/s
van Genuchten parameter α	1.9 m^{-1}	1.9 m^{-1}	1.9 m^{-1}
van Genuchten parameter β	6.0	6.0	6.0
Longitudinal dispersivity	0.0 m	0.0 m	1 m
Transverse dispersivity	0.0 m	0.0 m	0.1 m
Molecular diffusion coefficient	1.2×10^{-15} m^2/s	1.2×10^{-9} m^2/s	1.2×10^{-9} m^2/s

Table 3. Summary of Results for Tracer-Based Pre-event Contribution to Channel Outflow for the Hypothetical Flow System[a]

Simulation	Tracer-Based Subsurface Pre-event Contribution, %
Zero-dispersion	1.4
Diffusion-only	28.4
High-dispersion	37.4

[a]Percentage results are the pre-event contributions integrated over the 5-hour simulation period as interpreted from the simulated tracer concentrations.

topography height is used in the InHM model to account for water storage in the overland flow regime due to the presence of small topographic depressions below the scale of the mesh discretization and the mobile water depth is used such that overland flow ceases for overland flow depths less than the assumed value. For the high-dispersion case, longitudinal and transverse dispersivities of the groundwater tracer are 1.0 m and 0.1 m, respectively, while the longitudinal and transverse dispersivity values of the surface regime are both set to 0.1 m. The molecular diffusion coefficient for both tracers in the high-dispersion case is 1.2×10^{-9} m^2/s. For the diffusion-only case, the dispersivity values for both tracers are 0.0 m and the molecular diffusion coefficient is 1.2×10^{-9} m^2/s. For the zero-dispersion case, the dispersivity values for both tracers are 0.0 m and the molecular diffusion coefficient is 1.2×10^{-15} m^2/s. Care was taken to ensure that the grid was sufficiently fine to handle this latter case without producing spurious numerical oscillations in the concentrations.

[14] In this work the quantity of subsurface hydraulically driven groundwater flow contributing to streamflow is calculated by (1) setting the mechanical dispersion and diffusion parameters in InHM to zero and very low values, respectively, and (2) spatially integrating the InHM-calculated advective tracer fluxes entering the channel from the unsaturated and saturated zones for the two conservative tracers, one assigned an initial concentration of unity to the saturated zone water and another assigned an initial value of unity to the water in the unsaturated zone (if present) at each time step t. The use of very low dispersion parameters eliminates the influence of hydrodynamic dispersion/diffusion processes on the tracer signals of the water discharging from the system, such that the advective flux of each tracer corresponds to the water flux from each component's source water. Similarly, a third tracer assigned to the incoming rainfall can be used to track this component's contribution. We will refer to this procedure here as a hydraulically based separation procedure in order to differentiate it from the tracer-based hydrograph separation method based on (1a) and (1b). Moreover, because the hydraulically based method is able to track the spatial and temporal patterns of infiltrating/exfiltrating event water over the entire land surface, it represents an unambiguous methodology to compute the actual Darcian subsurface flow contributing to streamflow generation. Note that only a two-component separation is used in this section because the unsaturated zone is not involved, but a three-component methodology is used later in our interpretation of the Borden rainfall-runoff experiment [*Abdul*, 1985; *Abdul and Gillham*, 1989].

[15] For all three cases summarized in Table 3 and in Figure 2, a two-component version of (1b), which InHM can calculate directly, is used to perform a tracer-based estimate of the volume of pre-event water discharging from the system. For the zero-dispersion case, the contribution of pre-event water at the discharge point calculated from (1a) and (1b) was found to be 2.6 L (1.4% of the 192.5 L of water exiting the system) over the 5-hour simulation period. This quantity precisely agrees with our hydraulically based approach. Conversely, the estimated pre-event water contributions for the diffusion-only and high-dispersion cases that were calculated from (1a) and (1b) are 54.6 L (28.4%) and 71.9 L (37.4%), respectively (Table 3, Figure 2a). It should be noted that in all three scenarios, the total stream discharge, overland flow, and groundwater flow volumes remain constant because only the tracer dispersion param-

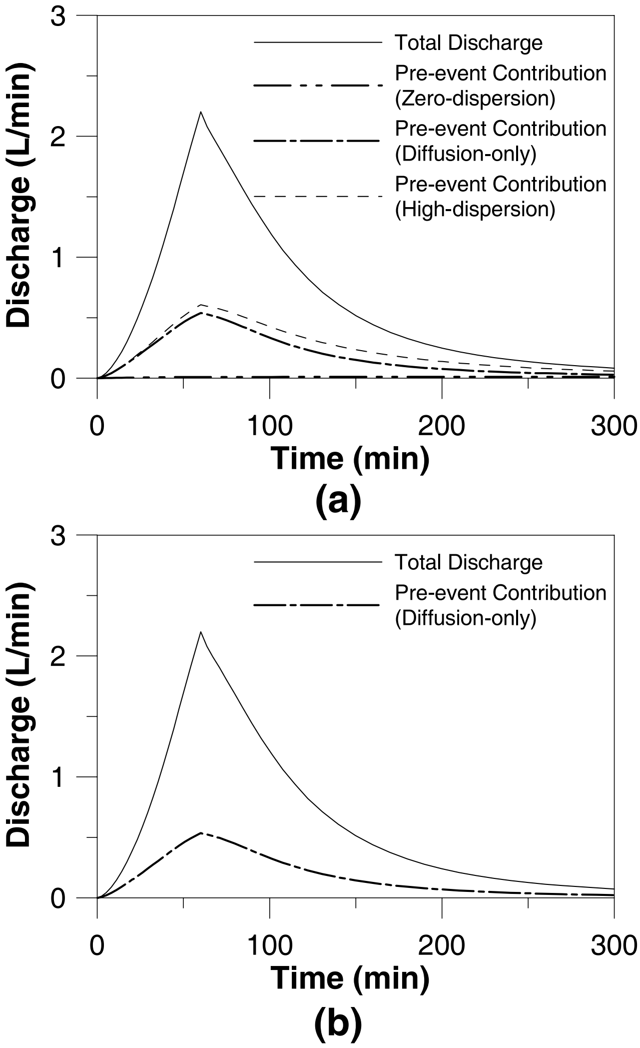

Figure 2. (a) A comparison between the tracer-based pre-event water contributions to the total stream discharge for three different dispersion cases outlined in Table 2. (b) The pre-event contribution calculated for the diffusion-only case but with effectively zero groundwater flow by reducing the saturated hydraulic conductivity by 2 orders of magnitude.

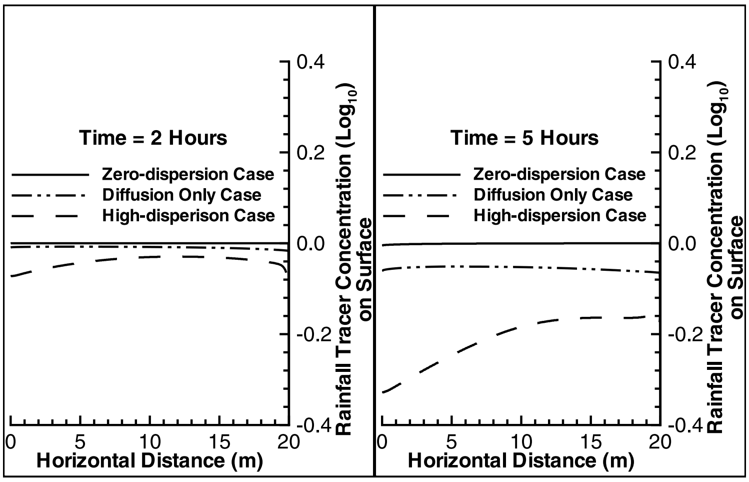

Figure 3. Rainfall tracer distributions on the land surface after 2 hours and 5 hours for the zero-dispersion, diffusion-only, and high-dispersion cases, respectively.

eters are altered. Additionally, as can be seen in Figure 3, the concentrations of the rainfall tracer along the land surface are essentially identical to its prescribed value of 1.0 after 2 hours for the zero-dispersion case, but have declined significantly with distance toward the discharge point for both the diffusion-only and high-dispersion cases. After 5 hours the rainfall-tracer concentrations for the zero-dispersion case remain close to 1.0 except for very near the discharge point. On the other hand, the rainfall-tracer concentrations across the surface have dramatically declined after 5 hours for the diffusion-only and high-dispersion cases. To further investigate how hydrodynamic mixing affects the pre-event contribution to streamflow estimated using a two-component version of (1b), an additional diffusion-only case was simulated in which groundwater contributions were effectively eliminated by setting the subsurface saturated hydraulic conductivity to a value 2 orders of magnitude lower (Figure 2b). For this case, the pre-event contribution to streamflow was calculated to be 27.7% (52.9 L) of the total discharge (191.0 L), even though the mechanical mixing and bulk groundwater flow quantities are negligible.

[16] The results from this conceptual example clearly demonstrate the major impact that hydrodynamic mixing can have on changing rainfall and groundwater tracer signatures along the surface and subsurface flow paths before discharging from the system. Thus, for flow regimes in which hydrodynamic mixing between different source-zone waters is nonnegligible, the values of Q_p, Q_u, and Q_s (or simply Q_p and Q_s for this example) determined from

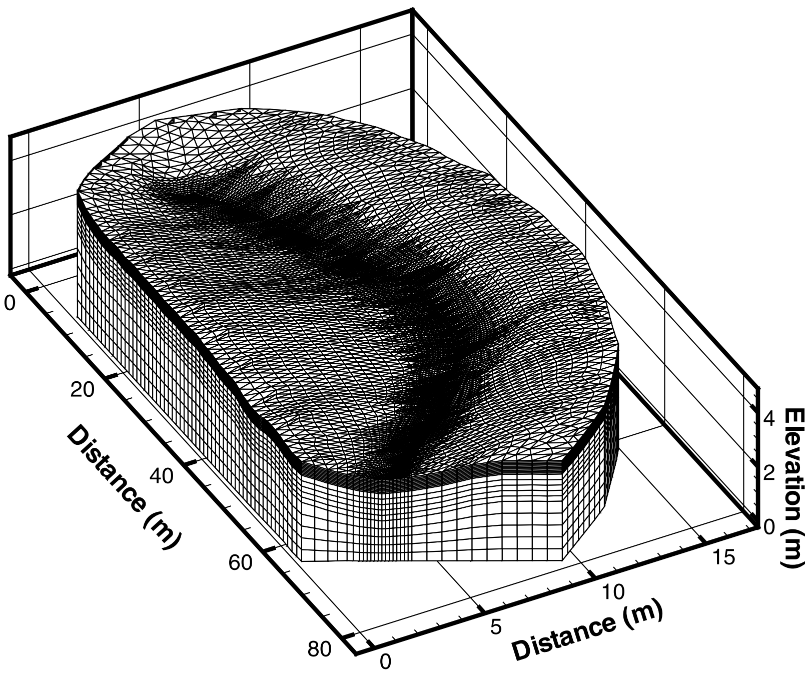

Figure 4. Finite element mesh of the Borden rainfall-runoff experiment. (Exaggeration = 1 × 3 × 4.)

Table 4. Surface and Subsurface Model Parameters Utilized in the Base-Case Simulation of the Borden Rainfall-Runoff Experiment

Parameter	Value
Surface	
Manning's roughness (channel)	0.03 s/m$^{1/3}$
Manning's roughness (slopes)	0.3 s/m$^{1/3}$
Microtopography height	1×10^{-2} m
Mobile water depth	1×10^{-4} m
Dispersivity (longitudinal and transverse)	0.1 m
Molecular diffusion coefficient	1.2×10^{-9} m^2/s
Subsurface	
Porosity	0.37
Specific storage	3.2×10^{-4} m^{-1}
Saturated hydraulic conductivity	1.0×10^{-5} m/s
van Genuchten parameter α	1.9 m^{-1}
van Genuchten parameter β	6.0
Longitudinal dispersivity	0.05 m
Transverse dispersivities	0.005 m
Molecular diffusion coefficient	1.2×10^{-9} m^2/s
Initial water table depth (below ground surface)	0.22 m

equations (1a) and (1b) will not correlate well with the actual hydraulic-gradient-driven components of flow they are commonly interpreted to represent. To further illustrate this point, we will examine the impact of hydrodynamic mixing on tracer-based hydrograph separations performed at a field site where a detailed and intensively monitored rainfall-runoff experiment was conducted.

4. The Borden Rainfall-Runoff Experiment

[17] The field site under consideration is a 0.1 ha experimental plot located within Canadian Forces Base Borden, approximately 70 km northwest of Toronto, Ontario. The area surrounding the plot has relatively low topographic relief, is covered by grass, and overlies a mildly heterogeneous aquifer composed primarily of medium sand. A constructed drainage channel that traverses the plot is about 60 cm wide and is grass-free. This site was the location of two intensively monitored rainfall-runoff experiments [*Abdul*, 1985; *Abdul and Gillham*, 1989]. The primary objective of the rainfall-runoff experiments was to assess the relative contribution of pre-event water to streamflow caused by the capillary-fringe effect during a rainfall event. One of the experiments involved applying an artificial rainfall event by irrigating the site at a rate of 2 cm/h for 50 min and subsequently allowing the system to drain. The experiment was monitored for an additional 50 min following the application of the artificial rainfall. A bromide tracer (90 mg/L) was added to the artificial rainfall water, thereby providing a means to differentiate the event from pre-event waters using a two-component, tracer-based hydrograph separation approach. The results indicated that the pre-event water comprised 37% of the total discharge volume measured in the channel [*Abdul*, 1985; *Abdul and Gillham*, 1989]. The rainfall-runoff experiment was unique in that the hydrogeological characteristics and antecedent hydrological parameters of the site were very well characterized and the experiment was both intensively instrumented and highly controlled.

[18] *VanderKwaak* [1999] successfully simulated the measured hydrograph for Borden rainfall-runoff experiment with the fully integrated InHM model and thus demonstrated its ability to represent the relevant physical processes contributing to streamflow generation at the subcatchment scale. In his numerical analysis, *VanderKwaak* [1999] utilized three independent, conservative tracers in the model simulations to tag the three different sources of water that contributed to the flow in the channel. First, a tracer concentration (i.e., bromide) was assigned to the rainfall to

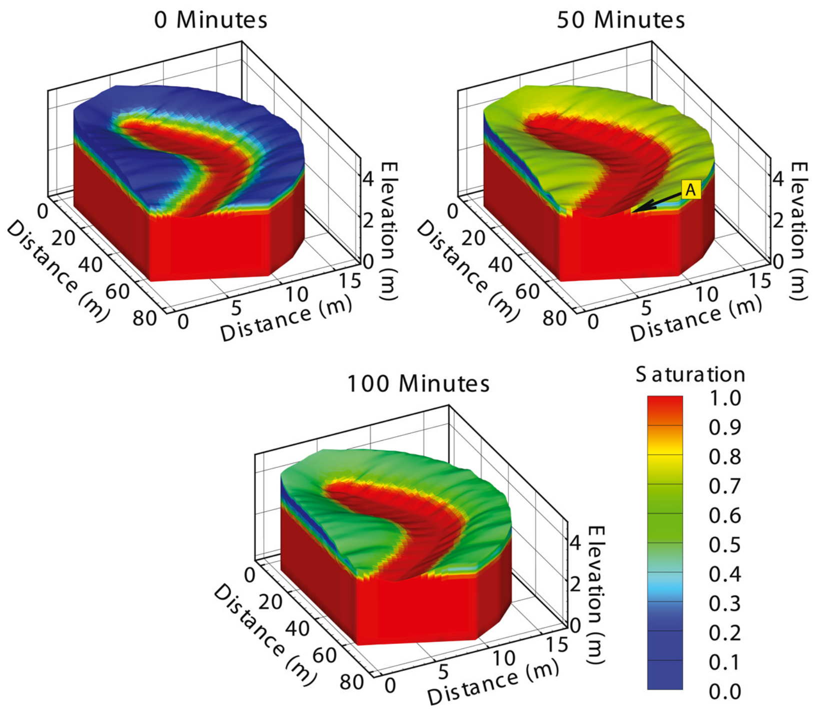

Figure 5. Water saturations after 0, 50, and 100 min. (Exaggeration = 1 × 4 × 8.)

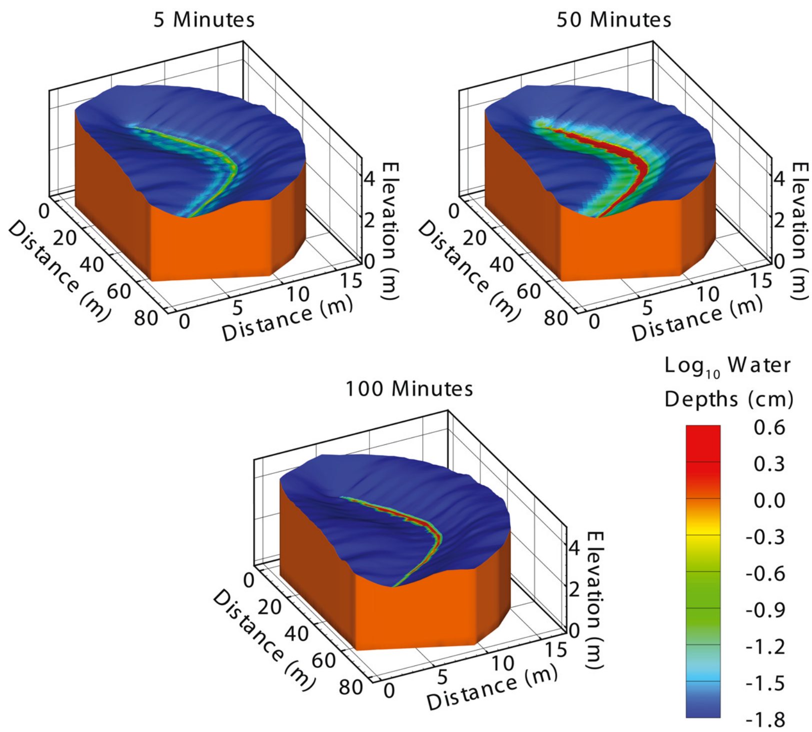

Figure 6. Surface water depths after 5, 50, and 100 min. (Exaggeration = 1 × 4 × 8.)

tag the movement and transport of the irrigated water. Second, two additional, independent tracers were assigned in the model to tag the pre-event waters initially stored in the unsaturated and saturated zones, respectively, prior to the initiation of the rainfall. This use of three different conservative tracers in the model was intended to make it possible to determine the relative contributions to the total streamflow from the precipitation (event), the saturated zone (pre-event), and the unsaturated zone (pre-event) waters as they migrated through the system and subsequently entered the channel. *VanderKwaak* [1999], however, did not explicitly separate the advective and dispersive/diffusive tracer contributions to the total solute fluxes entering the channel at each time step *t*. His estimated values of hydraulically driven subsurface contributions from the model results therefore represent the maximum possible contribution of water exfiltrating from the subsurface to generate streamflow because it would necessarily include the ongoing effect of dispersive/diffusive processes. By comparing the tracer-based estimate of the pre-event subsurface contribution using a separation procedure identical to that used by *Abdul* [1985] and *Abdul and Gillham* [1989] with the value computed from the summation of the unsaturated- and saturated-zone tracer fluxes discharging to the channel at each node in the finite element mesh, *VanderKwaak* [1999] found a significant discrepancy between these two types of estimates. Whereas the tracer-based pre-event contribution to the streamflow was estimated by *Abdul* [1985] and *Abdul and Gillham* [1989] to be approximately 37%, which agrees closely with the value computed by *VanderKwaak* [1999] from the InHM model results when the simulated bromide concentrations at the channel discharge point are entered into the mass balance equation (1b), the subsurface contribution obtained by summation of the nodal tracer fluxes was found to be much less. *VanderKwaak* [1999] suggested that this discrepancy could be the result of dispersive/diffusive mixing processes occurring at the surface-subsurface interface that, in turn, modified the tracer signals of the water being transmitted to the channel.

4.1. Comparison of Simulation Results With the Borden Rainfall-Runoff Field Experiment

[19] The numerical mesh used to discretize the physical setting is presented in Figure 4. The horizontal discretization is about 4 cm along the axis of the channel and gradually coarsens to approximately 50 cm in the upslope regions away from the stream. The vertical discretization is 5 cm for the first five layers adjacent to the land surface and increases to approximately 60 cm at depth. This fine level of discretization was chosen to minimize the impact of grid effects on the simulation results.

[20] The surface and subsurface parameters used in the base-case simulation are presented in Table 4 and are identical to those used by *VanderKwaak* [1999]. Zero-flux boundary conditions were assigned to both the lateral and bottom boundaries of the domain, and a nonlinear critical depth boundary condition was placed at the discharge point of the system. For the base-case simulation, rainfall was applied to the surface at a rate of 2.0 cm/h for 50 min and then the system was allowed to drain for an additional 50 min.

[21] The results presented in Figure 5 show the subsurface water saturations at times of 0, 50, and 100 min. Before the rainfall is initiated (0 min), the shallow subsurface

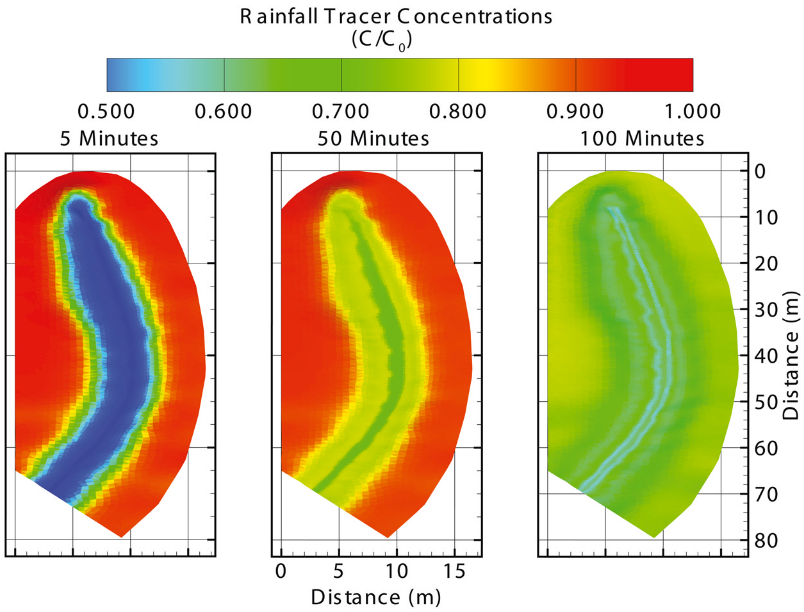

Figure 7. Surficial event-water tracer concentrations after 5, 50, and 100 min. (Exaggeration = 1 × 2.5.)

portion of the system is seen to be at residual saturation in the topographically higher regions, but is saturated near the channel where the capillary fringe of the water table intersects the land surface. After 50 min, which corresponds to the end of the rainfall event, the upland regions are now partially saturated and infiltration is occurring. At this time, the zone of high saturation has expanded significantly away from the channel and the water table has intersected the ground surface in this zone. The groundwater ridging due to the rapid rise in the capillary fringe can clearly be seen (point A in Figure 5). After 100 min, the system is still draining somewhat and the groundwater ridging effect has largely ceased.

[22] The surface water depths at 5, 50, and 100 min are shown in Figure 6. After 5 min into the rain event, water is beginning to pond in the channel, and after 50 min surface water depths in the flowing channel reach a maximum value of about 4.5 cm. This agrees with the field measurements. The water depths and flow rate in the channel have declined after 100 min, as expected.

[23] The event-water (rainfall) tracer concentrations on the land surface are presented in Figure 7 at 5, 50, and 100 min. After 5 min the event-water concentrations approach unity along the topographically higher regions of the surficial domain. Along overland flow paths approaching the channel, the concentrations of the event-water tracer decline, which is indicative of hydrodynamic mixing occurring due to the discharge of the pre-event tracers from the subsurface to the surface, mechanical dispersion, and molecular diffusion. The relative magnitude of this hydrodynamic mixing becomes even more pronounced in the regions immediately adjacent to and within the channel itself where the pre-event (saturated and unsaturated) tracers discharge to the surface at a more rapid rate. After 50 min, the zone of high event-water tracer concentration persists in the upslope regions, and the event-water tracer concentrations in the vicinity of the channel increase because the majority of the water ponding in the channel is now primarily composed of event-water runoff. After 100 min, the concentration of the event-water tracer is relatively uniform over the surficial domain except in the area immediately surrounding the channel axis where a small amount of subsurface seepage has further reduced the event-water concentrations. The changes in the concentration of the event-water tracer over the course of the simulation indicate that not only does there appear to be significant hydrodynamic dispersive/diffusive mixing occurring within the system, but also that the magnitude of this mixing varies over time.

[24] Figure 8 shows the distribution of event and pre-event tracer concentrations at the end of the simulation period in a transverse cross section taken at the approximate midpoint of the system. It can be seen that the penetration depths of the infiltrating event water are least in the mixing zone within and adjacent to the channel, but that upward migration of the pre-event, unsaturated-zone tracer in that same region is considerable, indicating that the event and unsaturated-zone pre-event waters are mixing with each other by means of dispersive/diffusive processes before discharging into the channel. Figure 8 also indicates that pre-event water originating from the saturated zone does not significantly contribute to streamflow generation because the saturated-zone tracer concentrations are low at the channel/subsurface interface. Nevertheless, the concentration gradients of the saturated-zone tracer are relatively large toward the stream channel.

[25] Figure 9 illustrates the transient response of the surface-subsurface water exchange fluxes across the land surface after 5, 50, and 100 min. Note that these water exchange fluxes are not specified parameters in InHM but instead evolve in space and time as a function of the local hydrodynamics. After 5 min into the rainfall event, it can be seen that event water is infiltrating into the subsurface over a substantial portion of the land surface except in the

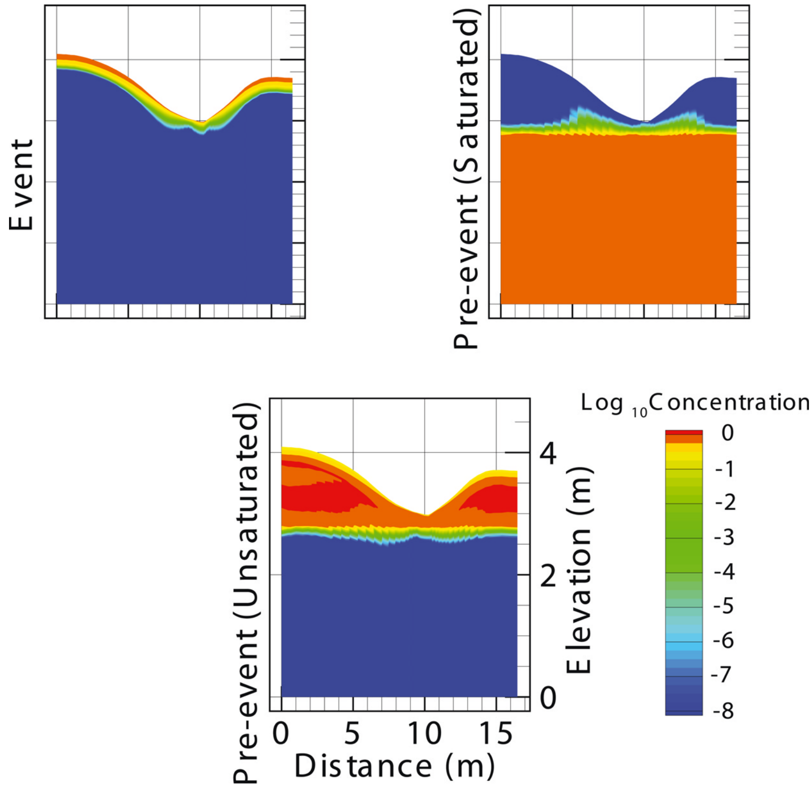

Figure 8. Saturated and unsaturated pre-event and event water tracer concentrations in a transverse cross section at the approximate midpoint of the system after 100 min. (Exaggeration = 1 × 4.)

immediate vicinity of the channel where subsurface discharge is occurring. After 50 min, infiltration continues away from the near-channel region and the subsurface discharge to the channel has increased in magnitude. The bright blue halo designating the zone of exfiltration surrounding the thalweg of the channel axis delineates the extent of the groundwater-ridging region. After 100 min, little or no water is being exchanged across the surface-subsurface interface with the exception of a small amount of exfiltration that is occurring within the channel.

[26] Figure 10 shows a comparison between the InHM-calculated and observed breakthrough curves of the total rate of bromide mass leaving the channel outlet. The rate of bromide-mass discharge is calculated by multiplying the concentration in the channel water by the flow rate at the outlet. The results are in good agreement, although the calculated curve peaks approximately 5 min later than the observed curve. The agreement suggests that the model is providing a reasonable representation of the dynamic flow and solute transport processes occurring in both the surface and subsurface flow regimes.

[27] A comparison between the observed and calculated discharge hydrographs is shown in Figure 11. As can be seen, the observed and calculated hydrographs show good agreement. Included in Figure 11 are the estimates of the pre-event subsurface contributions to the discharge hydrograph calculated from the simulated values of the event-water tracer concentrations at the channel discharge point using the tracer-based approach for hydrograph separation. Also shown is the estimated pre-event contribution calculated by *Abdul* [1985] and *Abdul and Gillham* [1989] using the actual measured bromide concentrations and the tracer-based approach for separation. Although the peak for the simulated pre-event contribution lags that based on the measured data by approximately 5 min, the agreement is reasonable. The tracer-based separation based on the model results indicates that about 35% of the total outflow is composed of pre-event water, which is comparable to the 37% contribution found by *Abdul* [1985] and *Abdul and Gillham* [1989].

[28] The ability of the InHM model to reasonably match both the measured hydrograph and the measured bromide-mass breakthrough curve builds confidence in the model's ability to capture the salient flow and tracer transport processes in both the surface and subsurface regimes. We have also seen from the results provided in Figure 11 that the volume of pre-event water contributed to the hydrograph that was estimated from the simulated bromide concentrations match *Abdul*'s [1985] estimate reasonably well; however, the quantity of subsurface flow entering the channel, calculated by the hydraulically based procedure, is only about 1.7% of the total streamflow discharge. This discrepancy between the estimates of the tracer-based pre-event contribution and the hydraulically based volume of subsurface flow contributing to streamflow is also shown in Figure 11. This level of disagreement between the tracer-based and hydraulically based separations reinforces the hypothesis that hydrodynamic mixing can lead to a significant inflation of the pre-event contribution estimated from tracer data when the data are interpreted with mass balance

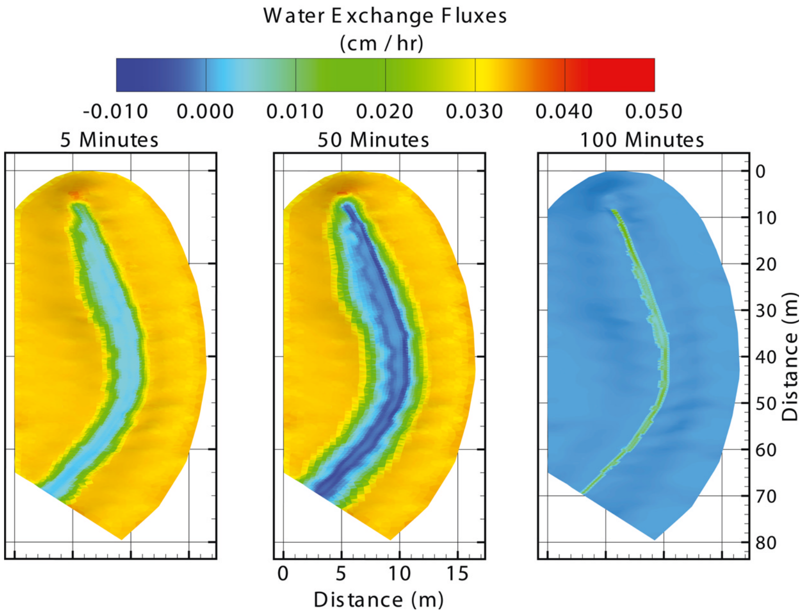

Figure 9. Surface-subsurface water exchange fluxes across the land surface interface after 5, 50, and 100 min. (Exaggeration = 1 × 2.5.)

relationships such as (1b) that lump advective and dispersion/diffusive transport processes.

4.2. Analysis of the Impact of Hydrodynamic Mixing

[29] In this section, factors that can influence the degree of hydrodynamic mixing between the event and pre-event waters are varied from their initial base-case values as described earlier. This is done to further demonstrate the impact of dispersive/diffusive mixing processes along surface and subsurface flow paths and the impact of this mixing on a traditional tracer-based hydrograph separation. Specifically, the influence of subsurface longitudinal dispersion, rainfall intensity/duration, and multiple sequential rainfall events are examined in the context of the Borden rainfall-runoff experiment. In all of the scenarios presented below, the pre-event contributions to the total discharge estimated using the tracer-based separation method were found to be substantially larger than the hydraulically based values which represent the actual bulk flow of subsurface water into the stream, as summarized in Table 5. We remind the reader that the hydraulically driven flow volume for the subsurface component was only about 1.7% for the base case over the 100 min simulation period.

[30] As illustrated in Figure 12, an increase in the value of subsurface longitudinal dispersivity to 0.5 m from its base-case value of 0.05 m causes the estimate of the tracer-based pre-event contribution to increase noticeably. Alternatively, if the subsurface longitudinal dispersivity value is decreased to 0.005 m, also shown in Figure 12, the pre-event contribution estimated from the tracer-based approach decreases minimally. Moreover, it is apparent from Figure 12 that if the longitudinal dispersivity value was set to 0.0 m, thereby eliminating any mechanical mixing between the event and pre-event waters, the tracer-based interpretation would still be significantly greater than the hydraulically based subsurface contribution of about 1.7% due to the apparently strong influence of molecular diffusion on mixing. Note that the hydraulically based estimate of the pre-event contribution is identical to that shown in Figure 11 for the base case because a change in solute dispersion parameters does not affect the bulk flow of the aqueous phase.

[31] The influence of rainfall intensity/duration on tracer-based pre-event contributions was investigated by altering the rainfall event employed in the base case (i.e., 2.0 cm/h for 50 min) in two ways: (1) by increasing the rainfall intensity to 4 cm/h while decreasing its duration to 25 min (Figure 13) and (2) by decreasing rainfall intensity to 1.0 cm/h while increasing its duration to 100 min (Figure 14). Note that although the intensity of the rainfall in each of these

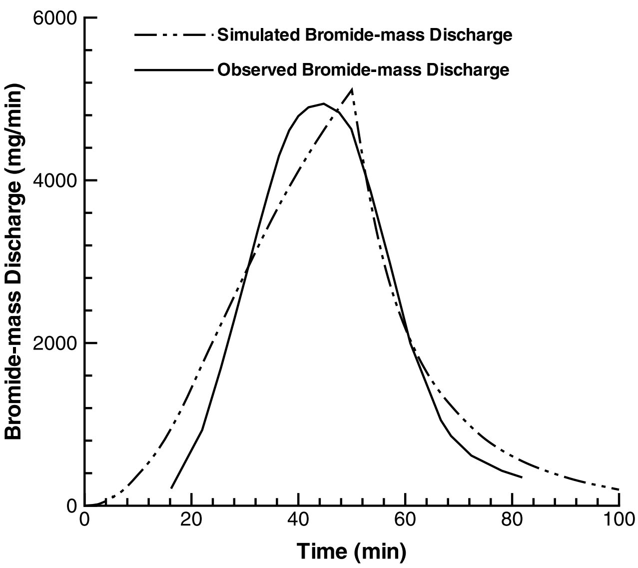

Figure 10. A comparison between the observed and InHM-calculated breakthrough curves for the bromide-mass discharge at the channel outlet.

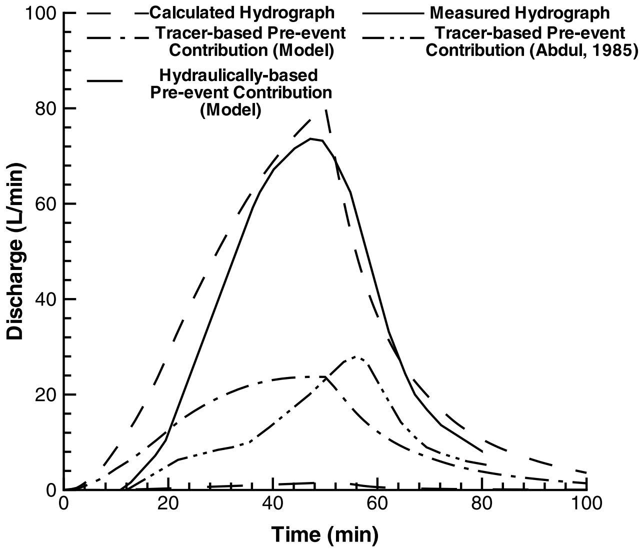

Figure 11. A comparison between the observed and InHM-calculated discharge hydrographs as well as the tracer-based and hydraulically based pre-event contributions.

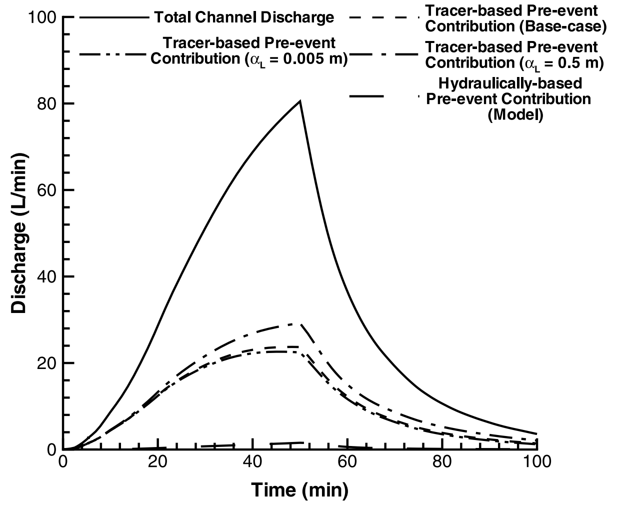

Figure 12. The effect of increasing and decreasing subsurface longitudinal dispersivity to 0.5 and 0.005 m, respectively, on the estimated pre-event contribution from the tracer-based separation.

simulations changes, its duration has also been altered such that the total volume of rainfall applied to the system remains identical to that of the base case. As is shown in Figure 13, increasing the rainfall intensity while decreasing its duration results in the discharge hydrograph peaking after 25 min and then slowly receding thereafter. Because the event and pre-event waters have less time to hydrodynamically mix by dispersion and diffusion before being transmitted to the channel when compared with the time available in the base case, it is expected that the influence of this mixing on the pre-event tracer signatures will be diminished. This will lead to a lower tracer-based pre-event contribution when contrasted to that of the base case. As can be seen in the summary provided in Table 5, this is indeed the case. Conversely, as is illustrated in Figure 14, decreasing the rainfall intensity while increasing its duration increases the amount of time available for hydrodynamic mixing and, as a consequence, results in a larger tracer-based estimate of the pre-event contribution (Table 5). Note that the hydraulically based estimates of the pre-event contributions are once again much lower than the tracer-based calculation. For the cases shown in Figures 13 and 14, the volumes of hydraulically driven pre-event water captured by the stream channel are only 0.7% and 2.5%, respectively.

[32] The impact of subjecting the system to multiple sequential rainfall events on the interpreted pre-event contribution using a tracer-based approach is shown in Figure 15. The intensity and duration of each of the rainfall events is identical to that of the base case and each event is separated by a 3-day recovery period. As Figure 15 illustrates, each sequential event yields a greater total channel discharge volume due to the progressively diminishing subsurface storage capacity. Intuitively one would expect that with the advent of each sequential rainfall event,

Table 5. Summary of Results for Tracer-Based Pre-event Contribution to Channel Outflow for the Borden Rainfall-Runoff Experiment[a]

Simulation	Tracer-Based Subsurface Pre-event Contribution, %
Base case	35.2
Longitudinal dispersivity = 0.5	41.6
Longitudinal dispersivity = 0.005	33.9
Increased rainfall intensity	29.9
Reduced rainfall intensity	39.8

[a]Percentage results are the pre-event subsurface contribution integrated over the 100 min simulation period as interpreted from the simulated tracer concentrations.

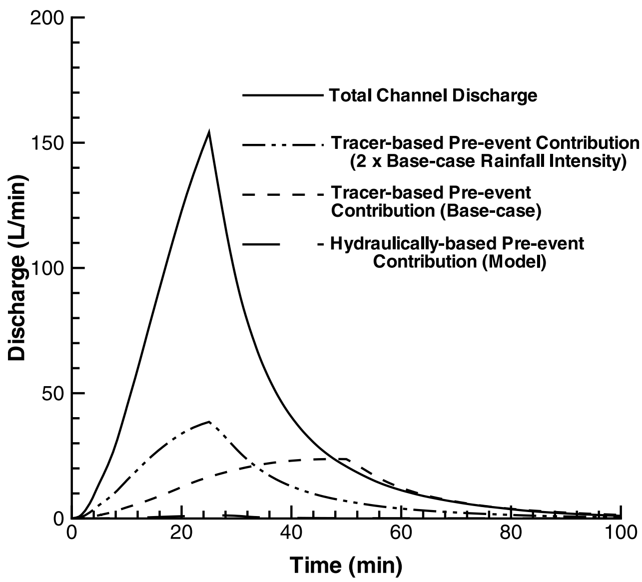

Figure 13. The effect of increasing rainfall intensity while decreasing its duration on the estimated pre-event contribution from the tracer-based separation.

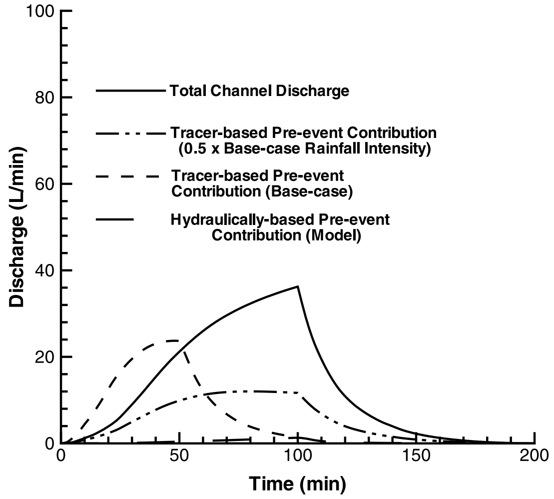

Figure 14. The effect of decreasing rainfall intensity while increasing its duration on the estimated pre-event contribution from the tracer-based separation.

progressively more of the original pre-event subsurface water would discharge from the system and subsequently be replaced by infiltrating event water. Therefore, if hydrodynamic mixing does influence pre-event water tracer signatures, then the tracer-based estimate of the pre-event contribution should decline with each sequential rainfall event. The summary provided in Table 6 shows this to be the case. For each of the events 1, 2, and 3 depicted in Figure 15, the hydraulically based pre-event contributions are 1.7, 2.5, and 3.8% of the total flow, respectively. With the advent of additional sequential events and recalling the relatively dry initial conditions, the hydraulically based contribution will eventually stabilize to a value of a few percent as the drainage and antecedent soil moisture conditions achieve a state of dynamic equilibrium. If the recovery period between each of these sequential rainfall events were to increase, there should also be a corresponding increase in the tracer-based interpretation of the pre-event contribution. This is confirmed by the 4-day recovery period case results presented in Table 6 when contrasted with those of the 3-day recovery period case. The converse argument can be made regarding the effect of decreasing the recovery period time.

5. Conclusions

[33] The preponderance of the geochemical evidence in the literature points to pre-event subsurface water as a major contributor to the increase in stream discharge observed during rainfall events in humid catchments. To date, there has been considerable debate in the scientific community as to which physical mechanisms are responsible for rapidly converting groundwater flow, which is generally considered to be a relatively slow process, into stream discharge. The

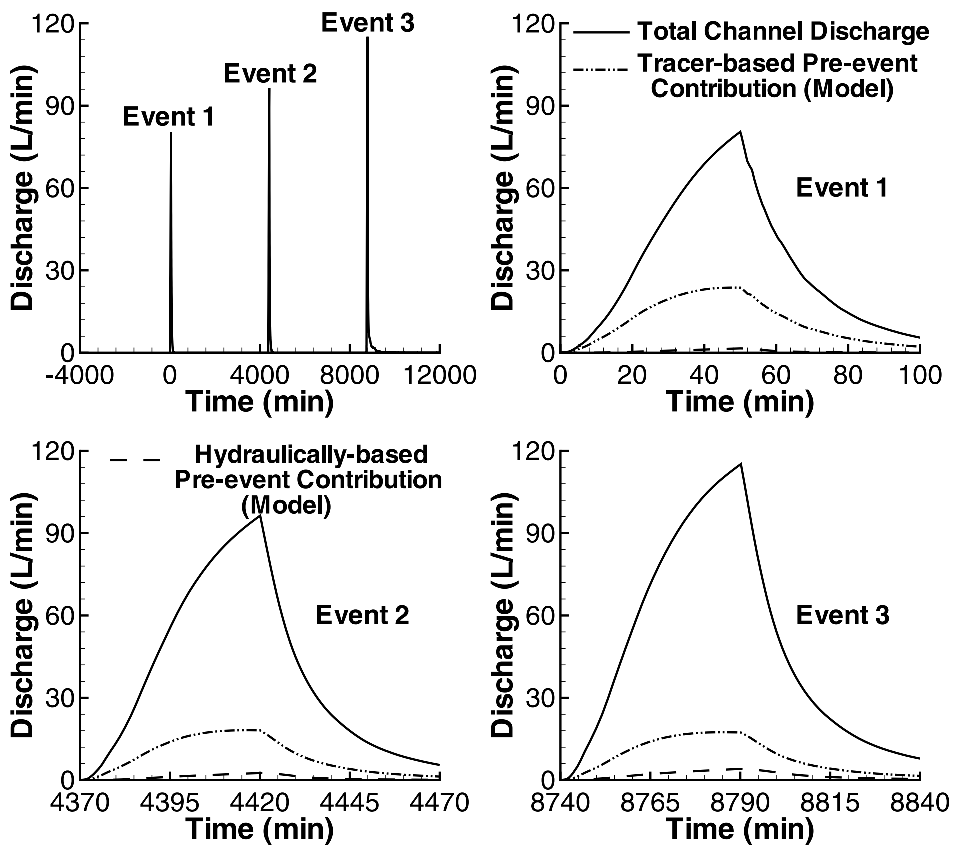

Figure 15. The effect of multiple sequential rainfall events on the estimated pre-event contribution from the tracer-based separation.

Table 6. Summary of Results for Tracer-Based Pre-event Contributions to Channel Outflow Under Multiple Sequential Rainfall Event Conditions

	Two-Day Recovery Period, %	Three-Day Recovery Period, %	Four-Day Recovery Period, %
Event 1	35.0	35.0	35.0
Event 2	21.0	22.4	23.3
Event 3	16.5	17.9	19.1

geochemical inference is based primarily on the results of tracer data, most of which are interpreted using mass balance equations such as those given by (1a) and (1b). Implicit in these mass balance equations is the assumption that hydrodynamic mixing processes such as mechanical dispersion and molecular diffusion are adequately accounted for in the calculation of the volumetric subsurface flow contributions. In light of the discrepancy between the conventional understanding of hydraulically driven flow processes and the inferences made from many tracer-test results, a question that arises is: Can the discrepancy be explained if hydrodynamic dispersion and the dispersive/diffusive exchange fluxes between the event and pre-event tracers are explicitly accounted for in the hydrograph separation procedure? Note that it is not the tracer test data themselves being questioned but, instead, the manner in which that data are interpreted.

[34] For all of the simulations performed in this work based on the Borden rainfall-runoff experiment, the pre-event contribution to the total discharge estimated using the tracer-based separation method was found to be substantially larger than the contribution determined by integrating the hydraulically driven subsurface flow components discharging into the surface-water channel. This difference was directly attributed to the impact of hydrodynamic dispersion on the mixing between event and pre-event tracers and because the dispersive/diffusive fluxes of each tracer entering the stream are not explicitly accounted for in the global mass balance equation (1b). Similar results were found with respect to the two-dimensional flow system presented in the illustrative example. It is recognized that the conclusions drawn here may not necessarily apply to all catchments; however, in catchments where both transient advective and dispersive/diffusive tracer fluxes play an important role, the event and pre-event tracer signatures can be altered significantly before being transmitted to the stream. In addition, the neglect of the dispersive/diffusive component of the total solute fluxes entering the stream will tend to inflate the tracer-based estimate of the volumetric contribution of pre-event water. If this is indeed the case, then the paradox of the rapid mobilization of old water is perhaps not paradoxical and that interpretations based on tracer-based hydrograph separation techniques should be reexamined with respect to their applicability for estimating hydraulically driven groundwater flow contributions to streamflow.

[35] **Acknowledgments.** We sincerely thank Joel VanderKwaak for providing technical support with regard to the InHM code and for his important contributions to this topic. We also greatly benefited from discussions with Frank Schwartz during his stay at Waterloo as the Walter Bean Visiting Professor. This work was funded by grants from the Natural Sciences and Engineering Research Council of Canada and the Canadian Water Network, and a Canada Research Chair in Quantitative Hydrogeology (Tier I) awarded to E. A. Sudicky. Additional funding was provided by grants 3-2-2 and 3-4-2 from the Sustainable Water Resources Research Center of the 21st Century Frontier Research Program of Korea.

References

Abdul, A. S. (1985), Experimental and numerical studies of the effect of the capillary fringe on streamflow generation, Ph.D. thesis, 210 pp., Univ. of Waterloo, Waterloo, Ont., Canada.

Abdul, A. S., and R. W. Gillham (1989), Field studies of the effect of the capillary fringe on streamflow generation, *J. Hydrol.*, *112*, 1–18.

Bishop, K. H., H. Grip, and A. O'Niell (1990), The origins of acid runoff in a hillslope during storm events, *J. Hydrol.*, *116*, 35–61.

Blowes, D. W., and R. W. Gillham (1988), The generation and quality of streamflow on inactive uranium tailings near Elliot Lake, Ontario, *J. Hydrol.*, *97*, 1–22.

Bottomley, D. J., D. Craig, and L. M. Johnston (1984), Neutralization of acid runoff by groundwater discharge to streams in Canadian Precambrian Shield watersheds, *J. Hydrol.*, *75*, 1–26.

Brown, V. A., J. J. McDonnell, D. A. Burns, and C. Kendall (1999), The role of event water, a rapid shallow flow component and catchment size in summer stormflow, *J. Hydrol.*, *217*, 171–190.

Burt, T. P. (2005), A third paradox in catchment hydrology and biogeochemistry: Decoupling in the riparian zone, *Hydrol. Processes*, *19*, 2087–2089.

Buttle, J. M. (1989), Soil moisture and groundwater responses to snowmelt on a drumlin hillslope, *J. Hydrol.*, *105*, 335–355.

Buttle, J. M. (1994), Isotope hydrograph separations and rapid delivery of pre-event water from drainage basins, *Prog. Phys. Geogr.*, *18*, 16–41.

Buttle, J. M., and D. L. Peters (1997), Inferring hydrological processes in a temperate basin using isotopic and geochemical hydrograph separation: A re-evaluation, *Hydrol. Processes*, *11*, 557–573.

Chanat, J. G., and G. M. Hornberger (2003), Modeling catchment-scale mixing in the near-stream zone: Implications for chemical and isotopic hydrograph separation, *Geophys. Res. Lett.*, *30*(2), 1091, doi:10.1029/2002GL016265.

Christophersen, N., and R. P. Hooper (1992), Multivariate analysis of stream water chemical data: The use of principal components analysis for the end-member mixing problem, *Water Resour. Res.*, *28*(1), 99–107.

Christophersen, N., C. Neal, and R. P. Hooper (1990), Modeling streamwater chemistry as a mixture of soil water end-members, a step towards second generation acidification models, *J. Hydrol.*, *116*, 307–320.

Crouzet, E., P. Hubert, P. Olive, E. Siwertz, and A. Marce (1970), Le tritium dans les measures d'hydrologie de surface: Determination experimentale du coefficient de ruissellement, *J. Hydrol.*, *11*, 217–229.

DeWalle, D. R., B. R. Swistock, and W. E. Sharpe (1988), Three-component tracer model for stormflow on a small Appalachian forested catchment, *J. Hydrol.*, *104*, 301–310.

Fritz, P., J. A. Cherry, K. U. Weyer, and M. Sklash (1976), Storm runoff analyses using environmental isotopes and major ions, in *Interpretation of Environmemtal Isotope and Hydrochemical Data in Groundwater Hydrology*, pp. 111–130, Int. At. Energy Agency, Vienna, Austria.

Genereux, D. P., and R. P. Hooper (1998), Oxygen and hydrogen isotopes in rainfall-runoff studies, in *Isotope Tracers in Catchment Hydrology*, edited by C. Kendall and J. J. McDonnell, pp. 319–346, Elsevier, New York.

Gillham, R. W. (1984), The capillary fringe and its effects on water-table response, *J. Hydrol.*, *67*, 307–324.

Hewlett, J. D., and A. R. Hibbert (1967), Factors affecting the responses of small watersheds to precipitation in humid areas, in *International Symposium on Forest Hydrology*, edited by W. E. Sopper and H. W. Lull, pp. 275–290, Elsevier, New York.

Hill, A. R., and J. M. Waddington (1993), Analysis of storm run-off sources using oxygen-18 in a headwater swamp, *Hydrol. Processes*, *7*, 305–316.

Hooper, R. P. (2001), Applying the scientific method to small catchment studies: A review of the Panola Mountain experience, *Hydrol. Processes*, *15*, 2039–2050.

Hooper, R. P. (2003), Diagnostic tools for mixing models of stream water chemistry, *Water Resour. Res.*, *39*(3), 1055, doi:10.1029/2002WR001528.

Hooper, R. P., N. Christophersen, and N. E. Peters (1990), Modelling streamwater chemistry as a mixture of soilwater end-members: An application to the Panola mountain catchment, Georgia, U.S.A., *J. Hydrol.*, *116*, 321–343.

Jordan, J. P. (1994), Spatial and temporal variability of storm flow generation processes on a Swiss catchment, *J. Hydrol.*, *153*, 357–382.

Kendall, C., J. J. McDonnell, and W. Gu (2001), A look inside the "black box" hydrograph separation models: A study at the Hydrohill catchment, *Hydrol. Processes*, *15*, 1877–1902.

Kennedy, V. C., C. Kendall, G. W. Zellweger, T. A. Weyman, and R. J. Avenzino (1986), Determination of the components of stormflow using water chemistry and environmental isotopes, Mattole River Basin, California, *J. Hydrol.*, *84*, 107–140.

Kirchner, J. W. (2003), A double paradox in catchment hydrology and geochemistry, *Hydrol. Processes*, *17*, 871–874.

Leopoldo, P. R., and J. C. Martinez (1987), Runoff hydrograph analysis in agricultural watersheds by oxygen-18, in *Simposio Internacional Sobre el Empleo de Tecnicas Isotopicas Para el Aprovechamiento do Recursos Hidricos*, pp. 200–217, Int. At. Energy Agency, Vienna, Austria.

Loye-Pilot, M. D., and C. Jusserand (1990), Decomposition chimique et isotopique d'un hyrdrogramme de crue d'un torrent mediterraneen—Reflexions methodologiques, *Rev. Sci. Eau*, *3*, 211–231.

McDonnell, J. J. (1990), A rationale for old water discharge through macropores in a steep, humid catchment, *Water Resour. Res.*, *26*, 2812–2832.

McDonnell, J. J., M. Bonell, M. K. Stewart, and A. J. Pearce (1990), Deuterium variations in storm rainfall: Implications for stream hydrograph separation, *Water Resour. Res.*, *26*(3), 455–458.

McGlynn, B. L., and J. J. McDonnell (2003), Quantifying the relative contributions of riparian and hillslope zones to catchment runoff, *Water Resour. Res.*, *39*(11), 1310, doi:10.1029/2003WR002091.

Mosley, M. P. (1979), Streamflow generation in a forested watershed, New Zealand, *Water Resour. Res.*, *15*, 795–806.

Nolan, K. M., and B. R. Hill (1990), Storm-runoff generation in the Permanente Creek drainage basin, west central California—An example of flood-wave effects on runoff compositions, *J. Hydrol.*, *113*, 343–367.

Novakowski, K. W., and R. W. Gillham (1988), Field investigations of the nature of water-table response to precipitation in shallow water-table environments, *J. Hydrol.*, *97*, 23–32.

Rice, K. C., and G. M. Hornberger (1998), Comparison of hydrochemical tracers to estimate source contributions to peak flow in a small, forested headwater catchment, *Water Resour. Res.*, *34*(7), 1755–1766.

Sklash, M. G. (1990), Environmental isotope studies of storm and snowmelt runoff generation, in *Process Studies in Hillslope Hydrology*, edited by M. G. Anderson and T. P. Burt, pp. 401–435, John Wiley, Hoboken, N. J.

Sklash, M. G., and R. N. Farvolden (1979), The role of groundwater in storm runoff, *J. Hydrol.*, *43*, 46–65.

Turner, J. V., and C. J. Barnes (1998), Modeling of isotope and hydrogeochemical responses in catchment hydrology, in *Isotope Tracers in Catchment Hydrology*, edited by C. Kendall and J. J. McDonnell, pp. 723–760, Elsevier, New York.

Turner, J. V., and D. K. MacPherson (1990), Mechanisms affecting streamflow and stream water quality: An approach via stable isotope, hydrogeochemical, and time series analysis, *Water Resour. Res.*, *26*(12), 3005–3019.

Turner, J. V., D. K. Macpherson, and R. A. Stokes (1987), The mechanisms of catchment flow processes using natural variations in deuterium and oxygen-18, *J. Hydrol.*, *94*, 143–162.

Turner, J. V., J. M. Bradd, and T. D. Waite (1991), The conjunctive use of isotopic techniques to elucidate solute concentration and flow processes in dryland salinized catchments, in *Proceedings of the International Symposium on Use of Isotope Techniques in Water Resources Development*, pp. 33–59, Int. At. Energy Agency, Vienna, Austria.

VanderKwaak, J. E. (1999), Numerical simulation of flow and chemical transport in integrated surface-subsurface systems, Ph.D thesis, 242 pp., Univ. of Waterloo, Waterloo, Ont., Canada.

VanderKwaak, J. E., and K. Loague (2001), Hydrologic-response simulations for the R-5 catchment with a comprehensive physics-based model, *Water Resour. Res.*, *37*(4), 999–1013.

Weiler, M., and F. Naef (2003), An experimental tracer study of the role of macropores in infiltration in grassland soils, *Hydrol. Processes*, *17*, 477–493.

A. E. Brookfield, J. P. Jones, Y.-J. Park, and E. A. Sudicky, Department of Earth Sciences, University of Waterloo, Waterloo, Ontario, Canada N2L 3G1. (sudicky@sciborg.uwaterloo.ca)